Colloids and Surfaces A: Physicochem. Eng. Aspects xxx (2012) xxx–xxx

Contents lists available at SciVerse ScienceDirect

Colloids and Surfaces A: Physicochemical and Engineering Aspects

journal homepage: www.elsevier.com/locate/colsurfa

On the relation between hierarchical morphology and mechanical properties of a colloidal 2D gel system

Davide Orsi[a], Giacomo Baldi[a,b], Pietro Cicuta[c], Luigi Cristofolini[a,*]

[a] Physics Department, University of Parma, Italy
[b] IMEM-CNR, Parma, Italy
[c] Cavendish Laboratory, University of Cambridge, UK

ARTICLE INFO

Article history:
Received 1 November 2011
Received in revised form 2 January 2012
Accepted 2 January 2012
Available online xxx

Keywords:
Langmuir monolayer
Interfacial Shear Rheometry
2D gel
Gold nanoparticles
Colloids

ABSTRACT

We study a bidimensional gel system formed by a Langmuir film of gold nanoparticles. Its morphology is thoroughly characterized by AFM, SEM, and ellipsometric imaging techniques and shows a complex structure with features on a hierarchy of different sizes following a Levy distribution. The mechanical response arising after the gel point is investigated by Interfacial Shear Rheometry. The film is found to be mainly elastic, with the mechanical moduli scaling as a power law of the reduced concentration, in the same way as the fluctuation time which was measured in a recent X-ray Photon Correlation Spectroscopy experiment. The frequency dependence of the moduli is well described in the framework of the Soft Glass Rheology model (SGR) [Sollich et al. Phys Rev Lett 78, 2020 (1997)]. In this theory a power law distribution of relaxation times is postulated, whose exponent is experimentally determined for the present case. Such a distribution may reflect – in the dynamics – the hierarchical nature of the morphology of the film evidenced by microscopy. A mastercurve can be built, extending time–temperature to a time–concentration superposition principle as in [Cicuta et al. Phys Rev Lett 90, 116103(2003)]. This allows to describe the mechanical response over a frequency range slightly larger than that experimentally accessible. Besides the SGR component, a viscous term is always present, whose origin is investigated also taking into account samples with different preparation histories.

1. Introduction

Many everyday life applications, as well as advanced technologies, rely on the diversity of colloidal interfacial processes and properties. In particular one of the frontiers in the field of nano sciences is represented by the self-assembling processes of molecules, colloidal particles and bio-colloidal materials at fluid–fluid interfaces, like in Pickering emulsions [1], and the possibility to tune their self-assembly properties [2]. In this framework, inorganic nanoparticles (NP) are particularly interesting as they can be exploited in an increasing number of technological applications, including biosensing, therapeutics [3,4] and diagnostics [5].

The basic scientific knowledge in this area feeds into many applications in chemical, pharmaceutical and food industries, as well as in designing nano-devices such as sensors, assays, photonics and bio-fuel cells. These devices in turn are deployed in the areas of energy, health and environmental protection. NPs can also be used as "additives" to improve the performance of existing materials (as thermal conductivity, mechanical stability or energy transfer) [6], or to impart new functions to them (e.g. magnetic NPs have been investigated for drug delivery [7,8]). From the fundamental point of view, NP bridge the length scales between molecular surfactants and micron-sized particles. The former usually are in dynamical equilibrium with a bulk reservoir, whereas the latter are irreversibly attached to the surface as first shown by Pieranski [9]. NPs are somehow in between the two extremes and can be in dynamical equilibrium between surface and subphase, depending on their coating and on surface pressure.

New experimental and theoretical tools need to be developed to address the complex and multidisciplinary issues raised from the study dynamics in confined geometry, such as on the interface. In particular, the interaction between nanoparticles at the interface (not directly predictable from their behaviour in solution) is of paramount importance in determining the properties of the interface itself. Recently Isa et al. have been able to characterize the adsorption of NPs at the oil–water interface [10] and to measure the contact angle at the microscopic interface between colloidal particles and fluid [11], which in turn determines the interaction between particles. Looking at the surface rheological properties, Cicuta et al. have been able to formulate a time/concentration superposition principle – analogue of the time/temperature superposition principle – to the case of the shear response of colloids at an interface [12]. This allows to build a mastercurve and thus to

* Corresponding author at: Physics Department, University of Parma, Parco Area delle Scienze 7/A, 43100 Parma, Italy. Tel.: +39 0521 905276; fax: +39 0521 905223.
E-mail address: Luigi.Cristofolini@fis.unipr.it (L. Cristofolini).

0927-7757/$ – see front matter © 2012 Elsevier B.V. All rights reserved.
doi:10.1016/j.colsurfa.2012.01.001

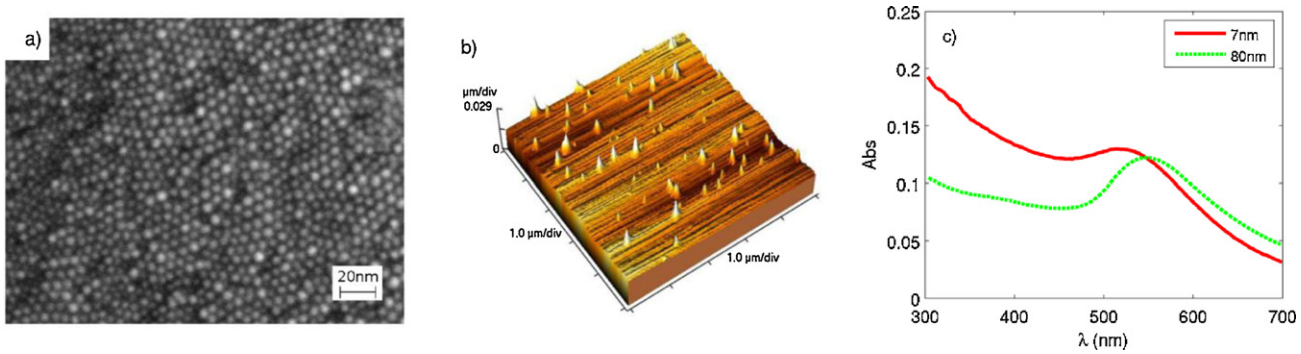

Fig. 1. Particle size is characterized by various techniques. (a) SEM image of an array of 7 nm diameter GNPs deposited on silicon substrate. (b) AFM image of the same nanoparticles spread on mica. (c) UV–Vis absorption spectrum from suspensions of GNPs of different sizes.

extrapolate the material response function outside the experimentally accessible frequency range. Optical techniques such as Waveguide Enhanced Dynamic Light Scattering [13] and Total Internal Reflection Ellipsometry [14] allow the study in situ of thin films in close proximity of solid surfaces, while X-ray Photon-Correlation Spectroscopy (XPCS) in total reflection mode [15,16] allows a direct measurement of the intermediate scattering function in the limit of long times, and to address the long-standing debate on the nature of dynamical heterogeneity in arrested systems. In principle the fluctuations measured on the microscopic scale by XPCS should be directly linked to those measured by interfacial microrheology techniques [17–19] and to the dissipation measured by Interfacial Shear Rheometry on the semi-macroscopic scale [20,21]. It is noteworthy that, even if the results of the different techniques agree on the qualitative evolution of the mechanical moduli as a function of thermodynamic parameters, there seem to be some important discrepancies in the absolute values of the moduli themselves. For example Ortega and co-workers measured the shear viscosity of a polymeric monolayer made of PtBA as a function of molecular weight, comparing the results of Multiple Particle Tracking and of oscillatory Interfacial Shear Rheometry. A difference was found of more than 3 orders of magnitude between the viscosities measured by the two techniques [19].

Therefore it is fair to say that, despite many efforts, the interfacial dynamics of colloidal nanoparticles is still far from being completely understood. In this paper we employ the semi-macroscopic technique of Interfacial Shear Rheometry to address the issue of the mechanical properties of a film of gold nanoparticles (GNPs) stabilized at the air water interface and we interpret our results in view of our recent characterization of surface fluctuations by XPCS [22]. We also show how the repulsive interaction that stabilizes the nanoparticles when suspended in an organic solvent, turns into an attractive interaction at the air/water interface.

2. Materials and methods

Gold nanoparticles coated by dodecanethiol have been produced following the literature [23] by Ruggeri and collaborators at the Chemistry Department of the University of Pisa, in the framework of an FP7 FET-OPEN project on Biologically Inspired Adaptive Organic Networks (BION). The nanoparticles have been thoroughly characterized by Dynamic Light Scattering, AFM, TEM and SEM microscopies. We report here some AFM images obtained using a Thermomicroscope Autoprobe CP Research instrument operated in contact mode with a SiN soft cantilever, and SEM images obtained by a FEG-SEM Zeiss Supra 40 operated at 2–10 kV. Null-ellipsometric imaging was performed either with an Optrel Multiskop operated at wavelength $\lambda = 632$ nm and by an EP3 Microscope produced by NANOFILM and operated at $\lambda = 532$ nm. Two different batches of colloids are used in the present study having diameter 7 nm and 80 nm, respectively, with typical distribution width $\sigma = 5$ and 20 Å. Their size has also been checked by measuring the UV–Vis absorption spectrum, which is shown in Fig. 1. Spectra were measured on a diluted hexane suspension of gold nanoparticles, using a double beam Jasco V-500 spectrometer. An estimation of the diameter, used to confirm the measurement obtained through SEM and TEM characterization, was evaluated from the position of the surface plasmon resonance peak of gold, following [24].

Uniform Langmuir monolayers have been prepared using an appropriate Langmuir trough with two moving barriers (maximum surface 280 mm × 80 mm). It must be noted that the dodecanethiol coating provides a hydrophobic interaction which stabilizes the particles when dispersed in an organic solvent (e.g. in toluene), so that the bulk suspensions are stable for months after preparation. On the contrary, when dispersed at the air/water interface, the same organic coating provides an attractive interaction between the particles, which then aggregate readily thus forming a very delicate branched 2D network structure which requires particular care in handling. Uniform Langmuir monolayers were prepared with an hexane–chloroform 9:1 suspension of gold nanoparticles, whose concentration was monitored by measuring its optical density. The suspension was spread on the water surface using a 50 μL Hamilton syringe, while keeping the tip of the needle in contact with the water surface. The spreading of a single syringe of solution required roughly 5 min, with frequent changes of the position of the needle's tip on the water surface. This was followed by a waiting time of 10 min for solvent evaporation. The procedure was repeated to reach the total amount of 400 μL of solution spread. Then the compression was started and successive very slow compression/expansion cycles were applied between the pressures of 3 and 5 mN/m, repeating the cycles at increasing pressure up to a maximum of 9 mN/m, at constant temperature of 15 °C, in a similar way as reported in the literature [25]. Measurements were then performed at constant temperature (18 °C) and increasing surface pressure, ranging from 10 mN/m up to 30 mN/m. In Fig. 2 we report a compression isotherm also containing a series of compression/expansion cycles, which produce an irreversible compaction of the Langmuir film. The required number of cycles (around 5) is empirically determined by observing when they do not produce a further increase of the packing of the film. In the presence of an important shear modulus, the surface pressure is to be replaced by the tensor of the stresses, and therefore the reading of Wilhelmy plate depends also on its relative orientation with respect to the moving barriers [26,27]. Keeping this in mind, the isotherms as well as all the rheological measurements presented in this work were performed while keeping the Wilhelmy plate always in the

Please cite this article in press as: D. Orsi, et al., On the relation between hierarchical morphology and mechanical properties of a colloidal 2D gel system, Colloids Surf. A: Physicochem. Eng. Aspects (2012), doi:10.1016/j.colsurfa.2012.01.001

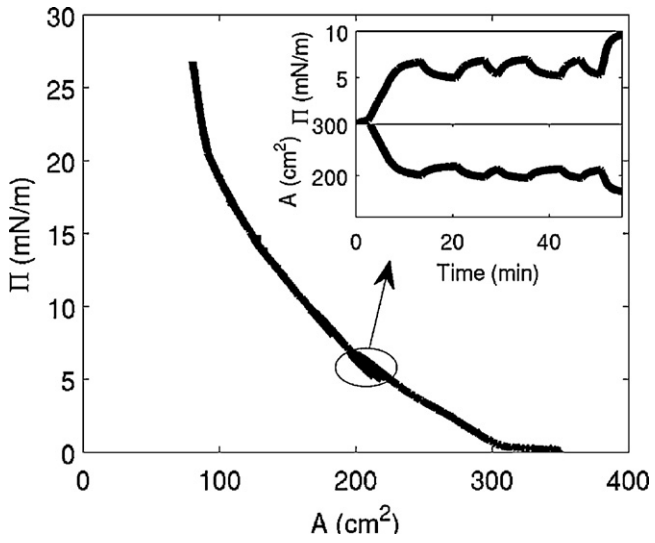

Fig. 2. Surface pressure–area compression isotherm for a 80 nm nanoparticle film. The surface layer of gold nanoparticles is initially prepared by a careful protocol of spreading and compression–expansion cycles. After the preparatory compression–expansion cycles used to improve the packing of the film, the surface pressure–area compression isotherm shows a clear upturn and a smooth build-up of pressure. Insets: time evolution of surface pressure Π and of the area A during the compression–expansion conditioning cycles.

same orientation, i.e. perpendicular to the moving barriers of the Langmuir trough.

The morphology of the monolayers thus obtained was characterized by null-ellipsometry in imaging mode, at wavelength $\lambda = 532$ nm, an example of which is shown in Fig. 3(a) and (b), in which a10× objective was used on monolayers of surface concentration $\phi = 31\%$ and $\phi = 71\%$, respectively. As the concentration is increased, an evolution from a foam-like structure, similar to what reported in [28], to a more compact structure can be observed. In Fig. 3(c) we report a SEM image of a monolayer of a similar concentration ($\phi = 69\%$) transferred onto solid substrate by the Langmuir Schaeffer technique. The marked similarity (although on different length scales) between Fig. 3(b) and (c) suggests that the transfer onto solid substrate do not substantially alter the film morphology.

A statistical analysis of this morphology, focusing on the size distribution of the voids in the film, is depicted in Fig. 3(d). The distribution follows a Levy distribution characterized by a long tail towards large voids described by an algebraic decay $N(d) \approx d^n$ with power coefficient $d = -3$ [22].

The fraction ϕ of area covered by nanoparticles is the main parameter controlling the properties of these films. In principle ϕ is deducible from the amount of dispersed suspension, but it has also been independently evaluated by imaging techniques to check for possible systematic errors. In Fig. 4 we compare, as a function of the surface area, the fraction ϕ deduced from the null-ellipsometric imaging (empty circles), and that obtained from SEM imaging of transferred monolayers at selected values of the area (filled circles) with the determination of ϕ from the dispersed amount (continuous line). The nice agreement between the different determinations makes us confident of their accuracy.

2.1. Mechanical measurements

Measurements of the mechanical properties of the film are done using an Interfacial Shear Rheometer (ISR). This instrument is an

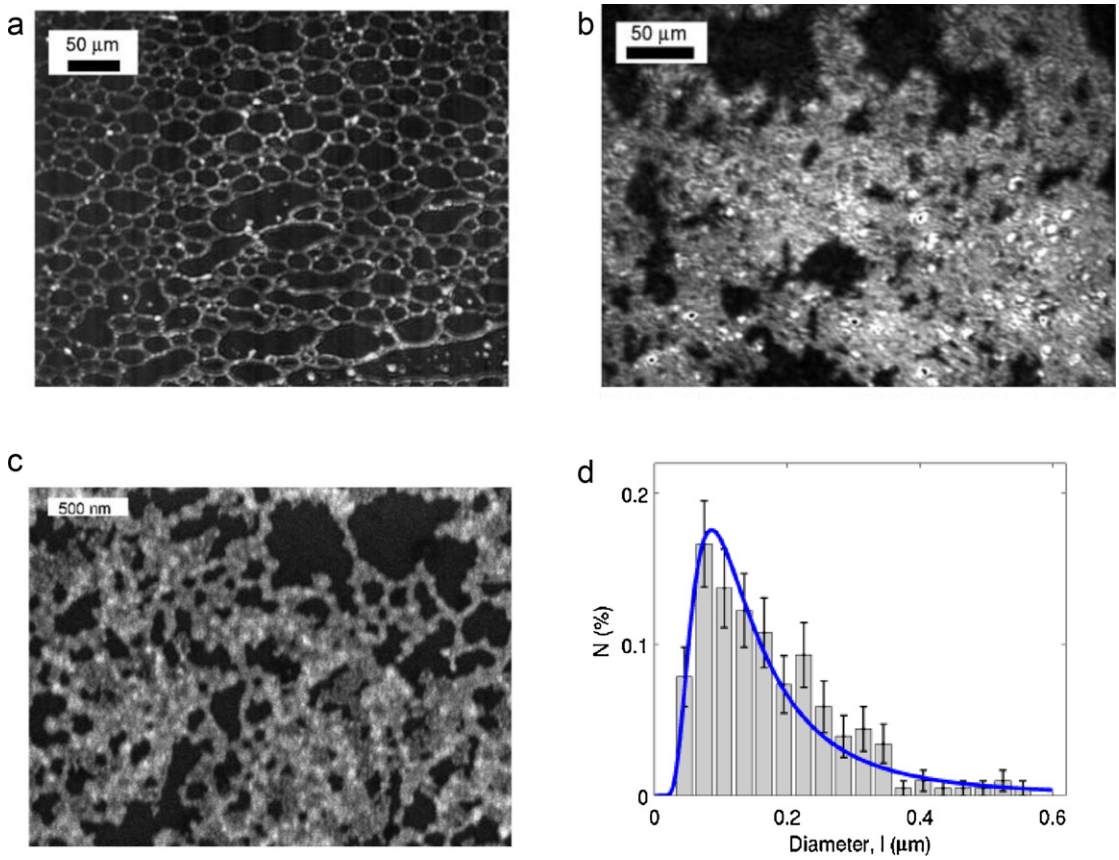

Fig. 3. The structure of the films is highly heterogeneous. (a) Null-ellipsometry imaging of a Langmuir monolayer at $\phi = 31\%$. (b) Null-ellipsometry imaging at $\phi = 71\%$. (c) SEM image of a monolayer deposited onto solid substrate at $\phi = 69\%$. (d) Levy distribution of void sizes following the Levy law discussed in the text.

Please cite this article in press as: D. Orsi, et al., On the relation between hierarchical morphology and mechanical properties of a colloidal 2D gel system, Colloids Surf. A: Physicochem. Eng. Aspects (2012), doi:10.1016/j.colsurfa.2012.01.001

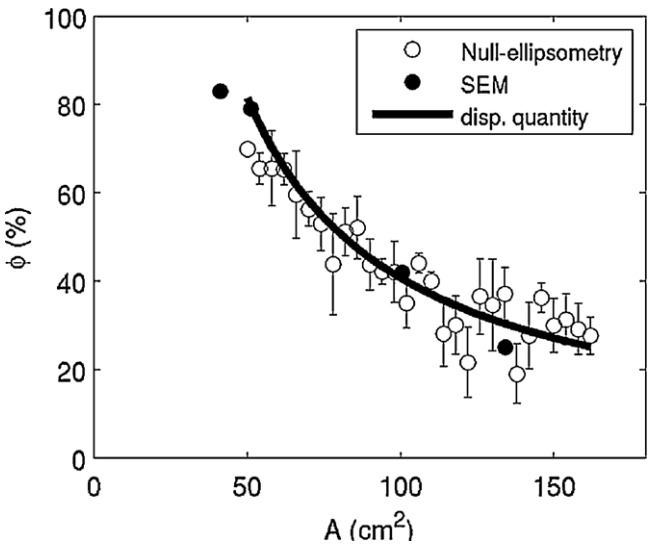

Fig. 4. There is agreement between three ways of measuring area fraction. Comparison of the determination of the covered fraction ϕ from the dispersed aliquot (continuous line) with that measured by null-ellipsometry imaging (empty circles) and by the analysis of the SEM images of samples deposited on solid substrate (filled circles).

adapted version of the device developed by Fuller and co-workers [20,21]. The probe consists in a needle (12 mm long, 0.34 mm thick) magnetized to saturation, that oscillates parallel to its axis on the water surfaces inside a channel, defined by two vertical parallel hydrophilic walls. Two coils in Helmholtz configuration (R = 16 cm), placed around the Langmuir trough, generate a constant field that aligns the needle along their axis, which lies on the water surface. A sinusoidal current with angular frequency ω is sent to one of the two coils to produce an oscillating field gradient that moves the needle, and assuming no-slip conditions, the same sinusoidal stress $\sigma(\omega)$ is induced on the monolayer. In this setup, the stress $\sigma(\omega)$ is proportional to half of the amplitude of the force exerted on the film, divided the length of the needle. The force is proportional to the sinusoidal tension applied to one coil, and the proportionality factor is obtained from a measurement of the oscillations on the water surface [20,29]. The resulting displacement of the needle is detected by a CCD USB camera (The Imaging Source, 1024 × 768 pixels) equipped with a long focal Mitutoyo MPLAN-APO-20X objective. The strain $\gamma(\omega)$ is measured as the amplitude of the needle oscillations divided by the distance between the needle and each wall of the glass channel in which it is floating. The shear strain $\gamma(\omega)$ induced on the film presents a phase lag with respect to the stress. The loss factor is then $\tan(\delta)$. An external trigger signal is used to synchronize the digital acquisition of both the image and the driving force, thus achieving a typical time accuracy better than 10 μs, required to properly determine the amount of elasticity of the film with respect to its viscosity. The complex dynamic shear modulus G^* describing the mechanical response of the film is then obtained from the relation:

$$G^* = G' + i * G'' = \frac{\sigma(\omega)}{\gamma(\omega)} e^{i\delta(\omega)} \quad (1)$$

in which G' and G'' are the storage and loss moduli, the real and imaginary parts of G^*. The instrument is capable of measuring mechanical moduli ranging from about 10 μN/m to about 100 mN/m covering the angular frequency range from 0.1 rad/s to 10 rad/s.

3. Results and discussion

In Fig. 5 we report the evolution of the dynamic shear modulus and of the loss factor (measured at $\omega = \pi$ rad/s) during compression of the Langmuir film at constant barrier velocity (diamonds and circles). It is noteworthy that the mechanical response of films formed by particles of either 7 nm and 80 nm diameter is mainly elastic even at the lowest concentration studied, meaning that a gel network has been formed. As the area is reduced, and the surface pressure increases, $|G|$ increases continuously while $\tan(\delta)$ shows little evolution, decreasing slightly and reaching a limit value close to 0.5. Therefore, the film is mainly elastic at almost all concentrations and this seems to be independent of the sample preparation, since it has been observed both in a film formed with the compression–expansion cycles and in a film formed without such a preliminary preparation (data not shown). This fact suggests that the behaviour of $\tan(\delta)$ is related with the interparticle interaction more than to the mesoscopic structure of the film. A similar evolution of mechanical moduli as a function of ageing time has been recently found in thermotropic colloidal gels [30]. On the contrary, the modulus $|G|$ clearly depends on the diameter of the particles, which is reasonable for a gel presenting formation of irreversible links during compression. We compare these results with measurements performed after a waiting time of 5 min following the end of the barrier's motion necessary to reach each surface

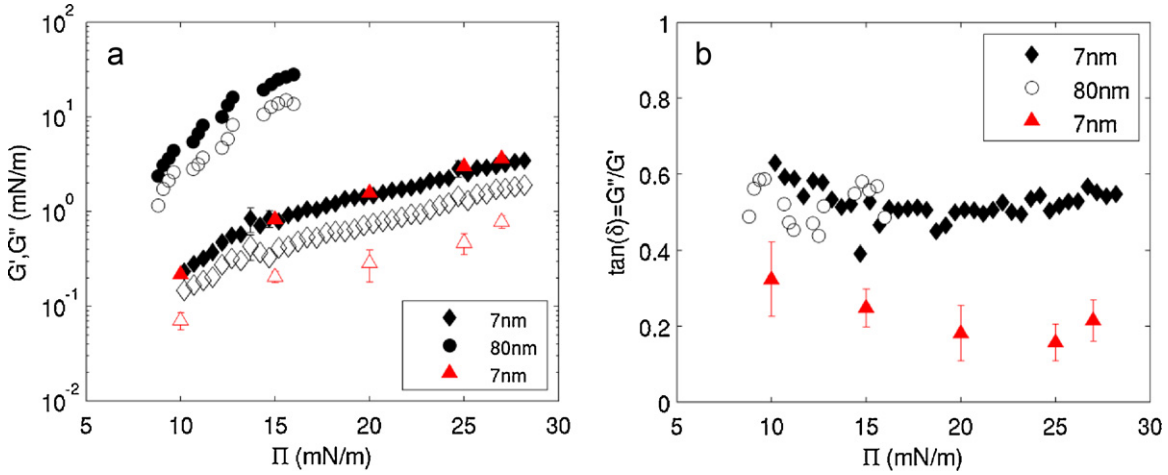

Fig. 5. The elastic component always dominates the response, and elasticity increases as the layer is compressed. (a) Mechanical shear moduli G' (filled symbols) and G'' (empty symbols) for Langmuir films of gold nanoparticles of 7 nm and 80 nm diameter measured at constant angular frequency ($\omega = \pi$ rad/s) both during compression of film (diamonds and circles for 7 and 80 nm, respectively) and after a waiting time (triangles). (b) Loss factor $\tan(\delta)$ measured in the same conditions.

Please cite this article in press as: D. Orsi, et al., On the relation between hierarchical morphology and mechanical properties of a colloidal 2D gel system, Colloids Surf. A: Physicochem. Eng. Aspects (2012), doi:10.1016/j.colsurfa.2012.01.001

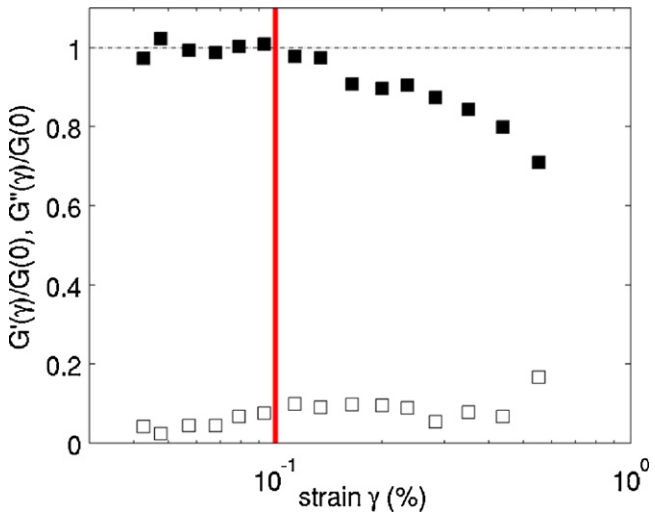

Fig. 6. Shear softening of the mechanical response for strain $\gamma > 0.1\%$. Dynamic shear moduli G' and G'', normalized to the limit of zero strain $|G(\gamma = 0)|$, measured as a function of the strain γ at constant $\omega = \pi$ rad/s.

pressure (red triangles). (For interpretation of the references to color in text, the reader is referred to the web version of this article.) We note that, while the storage modulus G' is unchanged, the loss modulus G'' (and so $\tan(\delta)$) is visibly reduced by a factor 2.5. This finding helps us in understanding the origin of the dissipation, which is to be related with the presence of dissipative "rubbing" motions between the particles, which is stronger when the system is much out of equilibrium (steady compression). This viscous mechanism is less pronounced when the system is allowed to relax towards a stationary gel state, waiting for some minutes after the end of the barrier motion.

Mechanical properties of gel systems are known to be strongly dependent on the strain amplitude, as at high deformation the gel mechanics can be non-linear: the breakage of weak links may alter the system and reduce the mechanical modulus. In order to check this point, we performed measurements as a function of the shear amplitude at a given frequency, namely $\omega = \pi$ rad/s, as shown in Fig. 6. We can identify a critical strain rate $\gamma' = 2 \times 10^{-3}$ s^{-1} as the limit below which the modulus is strain-rate independent. All the measurements reported here have been performed well below this threshold, in the linear regime.

The frequency dependence of G' and G'' is shown in Fig. 7(a) and (b). The storage modulus is almost constant in the frequency range here probed, with only a slight frequency dependence on the lower frequency side, which becomes more apparent at the highest covered fractions. The loss modulus is, on the contrary, almost constant at low frequency, crossing over to a linear increase at the higher frequencies. It should also be remembered that it remains always smaller than G'. This complex behaviour can be rationalized in the framework of a widely used model for the soft glass rheology (SGR) [31]. This viscoelastic model is an extension to the field of rheology of models, such as the trap model, commonly used in glass physics to describe systems under ageing [32]. The SGR model predicts that, in the linear regime, the system dynamics is governed by a distribution of relaxation times, $P(\tau)$, with a power law tail towards long times, $P(\tau) \sim \tau^{-x/x_g}$. Here x is an effective noise temperature and x_g a glass transition temperature, below which the system dynamics is time-dependent, in the sense that it is shows ageing. The model predict G' and G'' to follow, at sufficiently low frequencies, the same power law with an exponent $\alpha = (x/x_g) - 1$. In the same frequency range the loss factor, $\tan(\delta)$, is predicted to be proportional to α. Hence for small values of α the model is suitable to describe an essentially elastic material. In this framework the complex shear modulus is described by the following equations:

$$G' = A\omega^{\alpha} \tag{2}$$

$$G'' = B\omega^{\alpha} + \eta\omega$$

where $\alpha(\phi)$, $A(\phi)$, $B(\phi)$, $\eta(\phi)$ are the free parameters of the model. The purely viscous, or linear, term in G'' is not part of the SGR model itself: it is observed in many systems, and can be added to the model to account for the contribution coming from the suspension viscosity η, as in [33,34]. The continuous lines in Fig. 7(a) and (b) are obtained fitting simultaneously $G'(\omega)$ and $G''(\omega)$ for each measured packing fraction. The values of the exponent α range between 0.01 and 0.06, meaning that for all the packing fractions here studied the system is in a stationary state ($x > x_g$) but very close to the transition towards a situation where its dynamics would evolve with time. The ratio between the parameters B and A (the $\tan(\delta)$ of the SGR contribution) is always greater than 0.1 and almost constant as a function of the covered fraction, as shown in Fig. 7(c). We are thus confident that what we see is not an artifact of the measurement, since the ISR instrument is sensitive to such values of $\tan(\delta)$. The viscosity η increases with the surface concentration ϕ. This dependence is reported in Fig. 9 and is to be discussed later.

The frequency dependent mechanical moduli measured at several values of concentration ϕ, for either 7 nm and 80 nm nanoparticles, can be superposed to form a mastercurve. The superposition is obtained robustly – as a two step rescaling of each data set: the first step consists in a shift of both G' and G'' by the same factor b; the second step is done by multiplying the frequencies by a factor a. The master curves obtained are reported in Fig. 8. Since G' shows a very weak frequency dependence at all concentrations, the curves had to be shifted mainly along the y-axis. On the contrary, G'' presents the same decrease with ω at every value of ϕ,

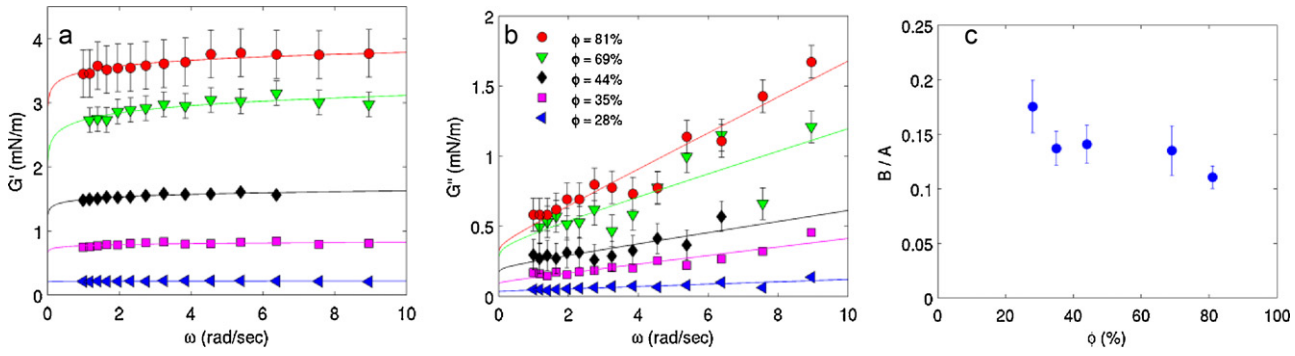

Fig. 7. Mechanical response of the system as a function of frequency. Mechanical shear moduli (a) G' and (b) G'' measured at increasing covered fraction as a function of the angular frequency. Lines are fit to Eq. (2), described in the text. (c) The loss factor of the SGR model – see Eq. (2) – reported as a function of surface concentration.

Please cite this article in press as: D. Orsi, et al., On the relation between hierarchical morphology and mechanical properties of a colloidal 2D gel system, Colloids Surf. A: Physicochem. Eng. Aspects (2012), doi:10.1016/j.colsurfa.2012.01.001

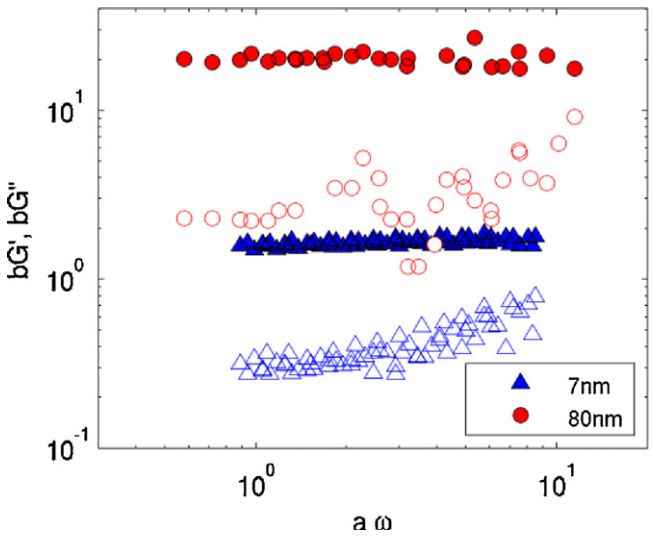

Fig. 8. Rheological master curves created from frequency-dependent measurement of the dynamic shear moduli. G' (filled symbols) and G'' (empty symbols) master curves for 7 nm (triangles) and 80 nm (circles) nanoparticle film, obtained from the scaling procedure described in the text.

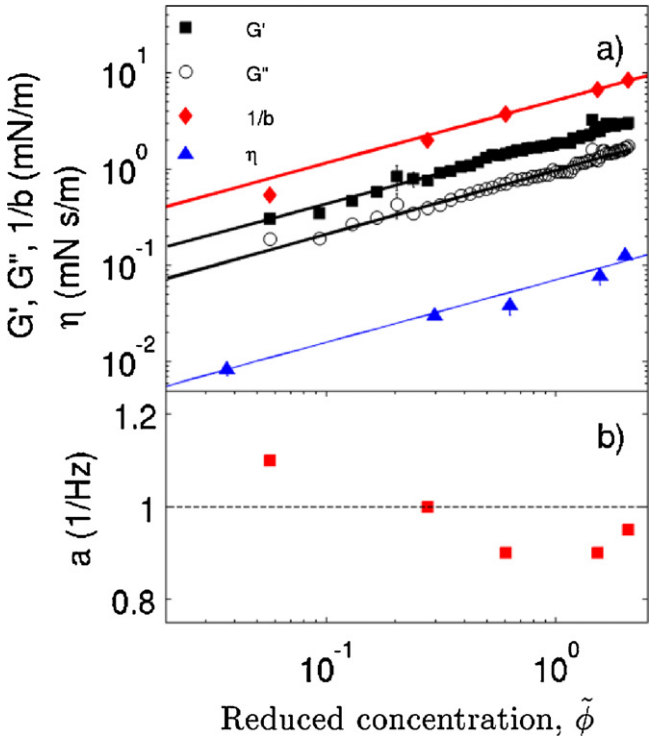

Fig. 9. The response moduli grow as a power law of the reduced concentration, after the gel point. (a) The dynamic shear moduli G' (squares) and G'' (circles), the inverse of the scaling parameter b used to build the master curve, and the effective viscosity η – measured for 7 nm nanoparticles – all follow the same functional dependence on the reduced concentration $\tilde{\phi}$. Continuous lines represent the power law fits to the data, with exponent $z = 0.65$. (b) The frequency re-scaling factor a is essentially independent of $\tilde{\phi}$.

therefore the parameter a – representing the shift along the x-axis – is constant over ϕ.

The scaling parameters a and b of the mastercurve are reported in Fig. 9 for the case of 7 nm nanoparticles at different concentrations. The frequency scaling parameter a is constant within the experimental accuracy. On the contrary, the mechanical shear moduli and the inverse of the scaling parameter $b(\phi)$, reported in Fig. 9(a), are found to obey a power law like $G' \propto \tilde{\phi}^z$ in which the power law exponent $z = 0.65(1)$ is the same for all the three quantities, and $\tilde{\phi}$ is the reduced concentration $\tilde{\phi} = (\phi - \phi_0)/\phi_0$, thus defined scaling the concentration to a reference value $\phi_0 = 0.27(1)$ close to that at which the gel was compacted by the expansion/compression cycles. Analogous results were found for films of 80 nm particles.

The power law scaling of elasticity post gel-formation has been shown in many bulk systems, and is related with the underlying physics of percolation [35,36]. The value of $z = 0.65$ measured here for the growth of two-dimensional G' is weaker than 2.4 observed in protein gels [37] or 4.0 in carbon black gels [38]. Both these systems however are in the bulk, and a dependence on dimensionality is to be expected. There is less comparable data in 2d, but approximately linear growth of G' for protein layers can be seen in [39].

One may wonder what is the meaning of ϕ_0: is it an intrinsic properties of the monolayer, a sort of minimal concentration for the formation of a percolation cluster, i.e. the threshold for the transition from viscous to elastic monolayer, or alternatively and more simply, ϕ_0 could be related with the sample preparation history. Further investigation is in progress also on films not compacted with any expansion/compression cycle, or compacted with cycles performed at higher surface pressure.

We note that the quantities reported in Fig. 9(a) – the storage and loss moduli, the inverse of the master curve parameter b, and the viscosity η deduced from the fits – all follow the same power law $G \propto \tilde{\phi}^{0.65}$ with $\phi_0 = 0.27$. This needs to be commented. The increase of G' – and correspondingly of $1/b$ – may result from the increase of adhesive links among the nanoparticles, which occurs with the increase of ϕ. Subsequently, the increase of G'' and of the effective viscosity η – which describe the linear dependence of $G''(\omega)$ – could indicate the onset of dissipation due to the increase of points of friction between nearest neighbours particles, which also can be thought to increase according with the number of links in the gel network.

4. Conclusions

We have here investigated complex interfacial systems constituted by bidimensional gels formed of nanometre sized particles, which bridge the gap between the more traditional Langmuir monolayers of surfactant molecules and those formed by micron-sized particles. The morphology of these systems has been thoroughly characterized by different microscopic techniques, namely AFM, SEM, and ellipsometric imaging. A combination of these techniques was needed in order to accurately determine the surface coverage fraction, which in turn is one of the parameters driving the mechanical properties of the film. The film shows a complex morphology with holes presenting a hierarchy of different sizes. The mechanical properties above the gel point are found to be dominated by the film elasticity, with the mechanical moduli scaling as a power law of reduced concentration. The reduced concentration is defined by scaling the effective concentration ϕ to a reference value ϕ_0 close to that at which the gel itself was formed. At the same time the frequency dependence of the complex modulus can be well described in the framework of Soft Glass Rheology, making reference to a wide distribution of relaxation times governed by a power law, which may reflect – in the dynamics – the fractal nature of the morphology of the film evidenced by microscopy. Well after the gel point, a viscous component is always present in the higher frequency region. Its origin is investigated also taking into account samples with different preparation histories. It is supposed that this dissipative response may originate from some mechanism of interparticle friction, as it scales with the surface coverage and therefore with the number of interparticle contacts, a quantity

Please cite this article in press as: D. Orsi, et al., On the relation between hierarchical morphology and mechanical properties of a colloidal 2D gel system, Colloids Surf. A: Physicochem. Eng. Aspects (2012), doi:10.1016/j.colsurfa.2012.01.001

whose growth is inferred from the elastic response. Finally, a mastercurve can be built, extending the well known time–temperature superposition to a time–concentration superposition principle and allowing to describe the mechanical response over a frequency range slightly larger than that experimentally accessible.

Acknowledgements

We would like to acknowledge Giacomo Ruggeri (Department of Chemistry, University of Pisa) for the GNP synthesis, Oleg Konovalov (Beamline ID10, ESRF, Grenoble) for the usage of ellipsometer in imaging mode, Tania Berzina (CNR-IMEM, Parma) for one of the SEM images and Yuri Gunanza (Parma) for the TOC artwork.

References

[1] B.P. Binks, T.S. Horozov (Eds.), Colloidal Particles at Liquid Interfaces, Cambridge University Press, Cambridge, 2006, p. 503.
[2] D. Wang, H. Duan, H. Möhwald, Soft Matter 1 (2005) 412.
[3] S. Lal, S.E. Clare, N.J. Halas, Accounts of Chemical Research 41 (2008).
[4] M. Namdeo, S. Saxena, R. Tankhiwale, M. Bajpai, Y.M. Mohan, S.K. Bajpai, Journal of Nanoscience and Nanotechnology 8 (2008) 3247–3271.
[5] W. Zhao, M.A. Brook, Y. Li, Chembiochem: A European Journal of Chemical Biology 9 (2008) 2363–2371.
[6] A.C. Balazs, T. Emrick, T.P. Russell, Science (New York, N.Y.) 314 (2006) 1107–1110.
[7] X. Zhao, J. Kim, C.A. Cezar, N. Huebsch, K. Lee, K. Bouhadir, D.J. Mooney, Proceedings of the National Academy of Sciences of the United States of America 108 (2011) 67–72.
[8] S. Erokhina, L. Cristofolini, T. Berzina, V. Erokhin, M.P. Fontana, Journal of Magnetism and Magnetic Materials 272–276 (2004) 1353–1354.
[9] P. Pieranski, Physical Review Letters 45 (1980) 569–572.
[10] L. Isa, E. Amstad, K. Schwenke, E. Del Gado, P. Ilg, M. Kröger, E. Reimhult, Soft Matter (2011) 7663–7675.
[11] L. Isa, F. Lucas, R. Wepf, E. Reimhult, Nature Communications 2 (2011) 438.
[12] P. Cicuta, E. Stancik, G. Fuller, Physical Review Letters 90 (2003).
[13] M.A. Plum, S.D.B. Vianna, A. Unger, R.F. Roskamp, H.-J. Butt, B. Menges, W. Steffen, Soft Matter 7 (2011) 1501.
[14] H. Arwin, M. Poksinski, K. Johansen, Applied Optics 43 (2004) 3028–3036.
[15] G. Grübel, A. Madsen, A. Robert, in: R. Borsali, R. Pecora (Eds.), Soft-Matter Characterization, Springer, 2008, pp. 935–995.
[16] D. Orsi, L. Cristofolini, M.P. Fontana, E. Pontecorvo, C. Caronna, A. Fluerasu, F. Zontone, A. Madsen, Physical Review E 82 (2010) 031804.
[17] M.H. Lee, S.P. Cardinali, D.H. Reich, K.J. Stebe, R.L. Leheny, Soft Matter (2011) 7635–7642.
[18] P. Cicuta, A.M. Donald, Soft Matter 3 (2007) 1449.
[19] A. Maestro, L.J. Bonales, H. Ritacco, T.M. Fischer, R.G. Rubio, F. Ortega, Soft Matter 7 (2011) 7761.
[20] C.F. Brooks, G.G. Fuller, C.W. Frank, C.R. Robertson, Langmuir 15 (1999) 2450–2459.
[21] S. Reynaert, C.F. Brooks, P. Moldenaers, J. Vermant, G.G. Fuller, Journal of Rheology 52 (2008) 261.
[22] D. Orsi, L. Cristofolini, G. Baldi, A. Madsen, submitted for publication.
[23] S. Chen, K. Kimura, Langmuir 15 (1999) 1075–1082.
[24] W. Haiss, N.T.K. Thanh, J. Aveyard, D.G. Fernig, Analytical Chemistry 79 (2007) 4215–4221.
[25] X.Y. Chen, J.R. Li, L. Jiang, Nanotechnology 11 (2000) 108.
[26] P. Cicuta, D. Vella, Physical Review Letters 102 (2009) 1–4.
[27] E. Aumaitre, D. Vella, P. Cicuta, Soft Matter 7 (2011) 2530.
[28] F. Bresme, M. Oettel, Journal of Physics: Condensed Matter 19 (2007) 413101.
[29] D. Orsi, L. Cristofolini, M.P. Fontana, Journal of Non-Crystalline Solids 357 (2011) 580–586.
[30] H. Guo, S. Ramakrishnan, J.L. Harden, R.L. Leheny, The Journal of Chemical Physics 135 (2011) 154903.
[31] P. Sollich, F. Lequeux, P. Hébraud, M. Cates, Physical Review Letters 78 (1997) 2020–2023.
[32] L. Berthier, G. Biroli, Reviews of Modern Physics 83 (2011) 587–645.
[33] A.J.C. Ladd, The Journal of Chemical Physics 93 (1990) 3484.
[34] T. Mason, D. Weitz, Physical Review Letters 75 (1995) 2770–2773.
[35] D. Stauffer, A. Coniglio, M. Adam, Advances in Polymer Science 44 (1982) 103–158.
[36] H.H. Winter, F. Chambon, Journal of Rheology 30 (1986) 367–381.
[37] A.M. Corrigan, A.M. Donald, Langmuir: The ACS Journal of Surfaces and Colloids 25 (2009) 8599–8605.
[38] V. Trappe, V. Prasad, L. Cipelletti, P.N. Segre, D.A. Weitz, Nature 411 (2001) 772–775.
[39] P. Cicuta, E.M. Terentjev, The European Physical Journal E, Soft Matter 16 (2005) 147–158.

Please cite this article in press as: D. Orsi, et al., On the relation between hierarchical morphology and mechanical properties of a colloidal 2D gel system, Colloids Surf. A: Physicochem. Eng. Aspects (2012), doi:10.1016/j.colsurfa.2012.01.001